ISSN 1070-3284, Russian Journal of Coordination Chemistry, 2016, Vol. 42, No. 12, pp. 789–796. © Pleiades Publishing, Ltd., 2016.

Three Metal Complexes Based on Tetrazolyl Ligands: Hydrothermal Syntheses, Crystal Structures, and Fluorescence Properties[1]

F. Wang[a, b], C. J. Wu[a], X. X. Liang[a], M. Y. Li[c], J. P. Li[a, *], and Z. Y. Liu[a, **]

[a] *College of Chemistry and Molecular Engineering, Zhengzhou University, Zhengzhou, Henan, 450001 P.R. China*

[b] *Department of Chemistry, Henan Institute of Education, Zhengzhou, Henan, 450014 P.R. China*

[c] *Zhengzhou Foreign Language High School, Zhengzhou, Henan, 450001 P.R. China*

**e-mail: ljp-zd@zzu.edu.cn*

***e-mail: liuzhongyi@zzu.edu.cn*

Received December 20, 2015

Abstract—Three new complexes based on 1-tetrazole-4-imidazole-benzene (Tibz), namely, $[Cd(Tibz)_2(H_2O)_2]_n$ (**I**), $[Mn(Tibz)_2(H_2O)_4] \cdot 2H_2O$ (**II**) and $[Co(Tibz)_2(H_2O)_4] \cdot 2H_2O$ (**III**) have been synthesized through hydrothermal method and structurally characterized by element analyses, IR spectroscopy and single-crystal X-ray diffraction analyses (CIF files CCDC nos. 1443867 (**I**), 1443868 (**II**), 1443869 (**III**)). Single-crystal X-ray diffraction reveals that complex **I** is a 1D double-chain architecture, **II** and **III** are both mononuclear complexes. The results of single-crystal X-ray diffraction analyses indicate that the hydrogen bond and π··· π stacking exist in the complexes, which make great contribution to the stabilities of complexes **I**–**III**. The fluorescent properties of these complexes have also been studied in the solid state at room temperature.

Keywords: synthesis, crystal structure, π···π interaction, fluorescence properties

DOI: 10.1134/S1070328416120071

INTRODUCTION

Recent years, the rational design and construction of metal-organic complexes have witnessed an upsurge of interest, not only because of their fascinating structures but also for their potential applications in catalysis, luminescence, ion exchange, molecular sensor technology, and so on [1–5]. It is well-known that the synthetic parameters, such as metal ions, ligands, solvent, pH, temperature, metal-to-ligand ratio have important influences on the self-assembly process of metal-organic complexes. Among them, the selection of suitable ligands is most critical. The rigidity, length, coordination modes or functional groups of organic ligands have important effects on the structures of MOFs. Nitrogen heterocyclic ligands, such as pyrazoles, imidazoles, triazoles and tetrazoles have been widely used due to their abundant coordination modes [6–10], and a variety of complexes with novel architectures and excellent properties have been successfully obtained. Especially, imidazole and tetrazoles have been extensively applied owing to the various coordination modes in the process of supramolecular assemblies [9, 10] and a large number of coordination polymers based on them have been reported [11]. However, there is no report on the use of 1-tetrazole-4-imidazole-benzene (Tibz), which contains imidazole and tetrazole functional groups as well. Meanwhile, it is an asymmetric ligand with the more abundant coordination groups which may give rise to intriguing supramolecular motifs and properties.

In this regard, three coordination complexes $[Cd(Tibz)_2(H_2O)_2]_n$ (**I**), $[Mn(Tibz)_2(H_2O)_4] \cdot 2H_2O$ (**II**) and $[Co(Tibz)_2(H_2O)_4] \cdot 2H_2O$ (**III**) were obtained by changing the metal ions and characterized by single-crystal X-ray crystallography, elemental analysis and infrared spectroscopy (IR). The results show that these complexes exhibit different structures though they were synthesized by the same method. Meanwhile, fluorescence properties of the complexes were studied and analyzed.

EXPERIMENTAL

Material and measurement. All chemicals were of analytical grade quality and purchased from commercial sources and used without further purification. IR data were recorded on a Nicolet NEXUS 470-FTIR spectrophotometer with KBr pellets in the range of

[1] The article is published in the original.

400–4000 cm^{-1} region. Elemental analyses (C, H, and N) were carried out on a Carlo-Reba 1106 elemental analyzer.

Synthesis of I. CdI_2 (18.3 mg, 0.05 mmol), Tibz (10.6 mg, 0.05 mmol), 5 mL of DMF (*N*,*N*-dimethylformamide), and 6 mL distilled H_2O were sealed in a 25 mL Teflon-lined stainless steel container and heated at 120°C for 3 days. After the mixture cooled to room temperature at a rate of 5 K/h. Finally, colorless block crystals were obtained in 66% yield.

For $C_{20}H_{18}N_{12}O_2Cd$

anal. calcd., %:	C, 42.08;	H, 3.18;	N, 29.44.
Found, %:	C, 42.10;	H, 3.19;	N, 29.40.

IR (KBr; ν, cm^{-1}): 3251 w, 3124 w, 1673 w, 1615 m, 1540 s, 1503 s, 1499 s, 1366 w, 1308 s, 1254 m, 1129 w, 1067 s, 1013 m, 964 m, 935 w, 835 s, 740 m, 648 s, 536 m, 487 m.

Synthesis of II. The procedure was the same to complex **I**, except that $MnCl_2 \cdot 4H_2O$ (9.9 mg, 0.05 mmol) replaced CdI_2. Finally, colorless block crystals were obtained in 69% yield.

For $C_{20}H_{26}N_{12}O_6Mn$

anal. calcd., %:	C, 40.89;	H, 4.80;	N, 28.61.
Found, %:	C, 40.92;	H, 4.86;	N, 28.63.

IR (KBr; ν, cm^{-1}): 3182 m, 1615 m, 1540 s, 1503 s, 1445 s, 1307 m, 1300 s, 1254 m, 1117 m, 1063 s, 964 m, 835 m, 760 m, 653 m, 487 s.

Synthesis of III. The procedure was the same to polymer **I**, except that $CoSO_4 \cdot 7H_2O$ (14.1 mg, 0.05 mmol) was used instead of CdI_2. Finally, red block crystals of **III** were obtained with a yield of 58%.

For $C_{20}H_{26}N_{12}O_6Co$

anal. calcd., %:	C, 40.90;	H, 3,65;	N, 28.70.
Found, %:	C, 40.89;	H, 3.76;	N, 28.70.

IR (KBr; ν, cm^{-1}): 3173 s, 1662 m, 1614.49 w, 1541.95 m, 1507 s, 1449 s, 1372 w, 1303 s, 1256 m, 1191 w, 1119 m, 1067 s, 1010 w, 963 m, 931 w, 841 s, 761 m, 724 w, 652 m, 529 w, 489 s, 427 w.

X-ray crystallography. The data of complexes **I**–**III** were collected on a Rigaku RAXIS-IV and SATURN-724 imaging plate area detector with graphite monochromated MoK_α radiation (λ = 0.71073 Å) at temperature of 293(2) K. The structures were solved by direct methods and refined with a full-matrix least-squares technique based on F^2. All calculations were performed using the SHELX-97 crystallographic software package [12]. The non-hydrogen atoms were refined anisotropically, while hydrogen atoms were generated geometrically. Table 1 shows crystallographic crystal data and structure processing parameters of **I**–**III**. Selected bond lengths and bond angles of **I**–**III** are listed in Table 2.

Supplementary material for structures **I**–**III** has been deposited with the Cambridge Crystallographic Data Centre (nos. 1443867 (**I**), 1443868 (**II**), and 1443869 (**III**); deposit@ccdc.cam.ac.uk or http://www. ccdc.cam.ac.uk).

RESULTS AND DISCUSSION

Single-crystal X-ray diffraction analysis reveals that polymer **I** has a 1D double chains architecture. As depicted in Fig. 1, the Cd(II) center is located in an inversion center and in a distorted octahedral geometry by coordinating to two oxygen atoms (O(1) and O(1*A*)) from two coordination water molecules, and four nitrogen atoms (N(1), N(1*A*), N(9) and N(9*A*)) from four Titb ligands, which is clearly centrosymmetric structure. The four nitrogen atoms are located in the equatorial plane, while the two oxygen atoms occupy the axial positions. The bond lengths of Cd(1)–N(1) and Cd(1)–N(9) are 2.3773 and 2.2573 Å, respectively. The Cd(1)–O(1) distance is 2.4533 Å. The Cd(1) is in the center of symmetry, and the equatorial plane deviation coefficient is 0.1061 Å. The angles between the equatorial ligands are all close to 90° (N(1)Cd(1)N(9) 89.471°).

The two ligands surround the metals to generate a 1D double chains structure, and the ligand-bridged Cd···Cd nonbonding distance is 11.0043 Å. Analysis of the crystal packing of **I** reveals that two adjacent 1D double chains are linked via interchain π···π stacking interactions between two adjacent parallel benzimidazole rings and imidazole rings with the inter-planar separations of 3.630 Å (center-to-center separation: 3.673 Å) (Fig. 1b) [13, 14]. More importantly, the two adjacent chains are also bridged through the stronger O–H···N hydrogen bonds for **I**, in which the hydrogen atoms come from the coordinated water molecular. In **I**, the H···N distances (bond angles) of the hydrogen bonds are 2.05 Å (171°) for O(1)–H(1*w*)···N(4) and 2.07 Å (170°) for O(1)–H(2*w*)···N(3). Both the above interactions extend the above 1D helical chains into 3D supramolecular framework (Fig. 1c).

Single-crystal X-ray diffraction analysis reveals that complexes **II** and **III** have similar structures and the same space group *C*2/*c* except that the central metal atom (Mn(II) for **II**, and Co(II) for **III**) are different. Complex **II** is a mononuclear architecture (Fig. 2a). The Mn^{2+} cation lies on a 2-fold rotation axis and it is in a distorted octahedral coordination environment in which four oxygen atoms (Mn(1)–

Table 1. Crystallographic data and structure refinement for complexes **I**–**III**

Parameter	Value		
	I	**II**	**III**
FW	510.63	585.47	589.46
Crystal system	Triclinic	Monoclinic	Monoclinic
Space group	$P\bar{1}$	$C2/c$	$C2/c$
a, Å	7.5830(15)	19.227(4)	19.059(3)
b, Å	8.0369(16)	13.142(3)	13.0652(6)
c, Å	9.1361(18)	13.409(3)	13.3483(16)
α, deg	102.80(3)	90	90
β, deg	97.57(3)	129.96(3)	129.49(2)
γ, deg	106.04(3)	90	90
V, Å^3	510.63(18)	2597.1(9)	2565.0(5)
Z	1	4	4
ρ_{calcd}, g cm^{-3}	1.856	1.497	1.526
F(000)	286	1212	1220
Crystal size	0.2 × 0.2 × 0.2	0.2 × 0.2 × 0.2	0.2 × 0.2 × 0.2
Index ranges *hkl*	$-9 \le h \le 9$, $-10 \le k \le 10$, $-10 \le l \le 11$	$-24 \le h \le 25$, $-17 \le k \le 17$, $-17 \le l \le 16$	$-22 \le h \le 23$, $-15 \le k \le 16$, $-13 \le l \le 16$
θ Range for data collection, deg	2.34–27.81	2.08–27.92	3.06–26.37
Reflections collected/unique	5736/2385	10711/3102	5663/2636
R_{int}	0.0345	0.0918	0.0630
Data/restraints/parameters	2385/2/168	3102/51/195	2636/28/195
Goodness-of-fit on F^2	1.255	1.017	1.041
Final R_1[a], wR_2[b] (all data)	0.0299, 0.1186	0.0796, 0.2112	0.0555, 0.1373
$\Delta\rho_{max}/\Delta\rho_{min}$, *e* Å^{-3}	0.823/–0.849	1.059/–0.550	0.652/–0.540

[a] $R_1 = ||F_o| - |F_c||/|F_o|$. [b] $wR_2 = [w(\left|F_o^2\right| - \left|F_c^2\right|)^2/w\left|F_o^2\right|^2]^{1/2}$. $w = 1/[\sigma^2(F_o)^2 + 0.0297P^2 + 27.5680P]$, where $P = (\left|F_c^2\right| + 2\left|F_c^2\right|)/3$.

Table 2. Selected bond lengths (Å) and angles (deg) for complexes **I**–**III***

Bond	*d*, Å	Bond	*d*, Å	Bond	*d*, Å
		I			
Cd(1)–N(9)$^{\#2}$	2.257(3)	Cd(1)–N(1)	2.377(3)	Cd(1)–O(1)	2.453(3)
		II			
Mn(1)–O(2)	2.190(3)	Mn(1)–N(1)	2.255(3)	Mn(1)–O(1)	2.207(3)
		III			
Co(1)–O(2)	2.121(3)	Co(1)–O(1)	2.123(2)	Co(1)–N(4)	2.144(3)
Angle	ω, deg	Angle	ω, deg	Angle	ω, deg
		I			
N(9)Cd(1)N(1)	89.47(11)	N(1)Cd(1)O(1)	81.17(10)	N(9)Cd(1)O(1)	94.52(10)
		II			
O(2)Mn(1)O(2)$^{\#1}$	87.34(17)	O(2)Mn(1)O(1)	90.84(12)	O(1)$^{\#1}$Mn(1)N(1)	99.83(13)
O(2)Mn(1)O(1)$^{\#1}$	80.87(12)	N(1)Mn(1)N(1)$^{\#1}$	94.34(18)	O(1)Mn(1)N(1)	87.98(13)
O(2)$^{\#1}$Mn(1)N(1)	168.54(13)	O(2)Mn(1)N(1)	90.20(12)		
		III			
O(2)$^{\#1}$Co(1)O(2)	170.35(15)	O(2)$^{\#1}$Co(1)O(1)	80.02(10)	O(1)Co(1)O(1)$^{\#1}$	86.15(14)
O(2)$^{\#1}$Co(1)N(4)$^{\#1}$	88.33(11)	O(2)Co(1)N(4)$^{\#1}$	98.21(11)	O(1)Co(1)N(4)$^{\#1}$	169.63(11)
N(4)$^{\#1}$Co(1)N(4)	94.94(17)	O(2)Co(1)O(1)	90.92(10)		

* Symmetry transformations used to generate equivalent atoms: $^{\#1}$ $-x, y, -z + 1/2$ for **II**; $^{\#2}$ $-x, y, -z + 1/2$ for **III**.

O(2) 2.1903, Mn(1)–O(1) 2.2073 Å) are from four coordination water molecules, and two nitrogen atoms (Mn(1)–N(1) 2.2553 Å) are from the imidazoles of the ligands. Unlike polymer **I**, the four atoms (N(1), N(1*A*), O(2) and O(2*A*)) lie in the equatorial plane with the bending angle of 15.976°, and two oxygen atoms (O(1) and O(1*A*)) are in apical positions. The bond angle of N(1)Mn(1)O(2*A*) is 168.541°, while the bond angle of O(1)Mn(1)O(1*A*) is 168.556°. In **III** (Fig. 3a), the central Co^{2+} ion lies on a 2-fold rotation axis and it is in a distorted octahedral coordination environment in which four oxygen atoms are from four coordination water molecules and two nitrogen atoms are from the imidazoles of the ligands. The bond length of Co–N is 2.144(3) Å, and the bond lengths of Co(1)–O(1) and Co(1)–O(2) are 2.123(2) and 2.121(3) Å, respectively, which is longer than those of $\{[Co(Tbta)(Pbdmbm)] \cdot 0.5H_2O\}_n$ (Pbdmbm = 1,10-(1,3-propanediyl)bis(5,6-dimethylbenzimidazole)] [15] and $[Co_2(Bib)_2(CA)_2] \cdot H_2O\}_n$ (Bib = 1,2-bis(imidazol-l-ylmethyl)benzene; H_2CA = camphanic acid) [16].

Analysis of the crystal packing of **II** and **III** reveals that there are stronger O–H···N and O–H···O hydrogen bonds between adjacent moleculars (Figs. 2b, 2c,

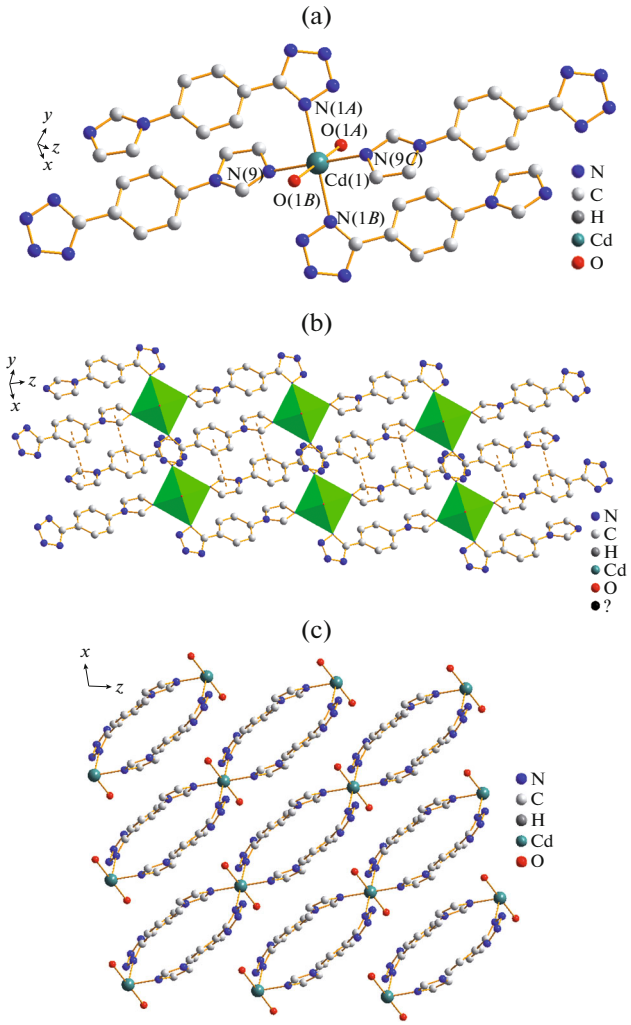

Fig. 1. The structure unit of **I** (a); the π···π stacking interactions (b); the packed structure of the polymer **I** (c). Hydrogen atoms are omitted for clarity.

3b, and 3c), in which the hydrogen atoms come from the coordinated or dissociative water molecules. In **II**, the H···O distances (bond angles) of the hydrogen bonds are 1.92 Å (152°) for O(2)–H(2*w*)···O(3) and 1.96 Å (165°) for O(2)–H(3)···O(3), while in **III**, the H···O distances (bond angles) of the hydrogen bonds are 1.9 Å (160°) for O(1)–H(1*B*)···O(3), which is in the normal ranges of O–H···O hydrogen bonds. In **II**, the H···N distances (bond angles) of the hydrogen bonds are 2.04 Å (165°) for O(1)–H(1)···N(5), 1.95 Å (167°) for O(3)–H(3*w*)···N(6), 1.91 Å (172°) for O(3)–H(3*wA*)···N(3) and 1.98 Å (166°) for O(1)–H(1*w*)···N(4), while in **III**, the H···N distances (bond angles) of the hydrogen bonds are 1.94 Å (172°) for O(3)–H(3*A*)···N(7), 2.02 Å (164°) for O(2)–H(2B)···N(2) and 1.92 Å (171°) for O(3)–H(3B)···N(8), which is in the normal ranges of O–H···N hydrogen bonds. In addition, there are π···π stacking interactions between two adjacent benzimidazole rings with the inter-planar separations of 3.47 (**II**) and 3.47 (**III**) (center-to-center separation: 3.78 (**II**) and 3.79 (**III**)). The adjacent mononuclear units are further linked together to form a infinite 3D architecture through these hydrogen-bonding interactions (Fig. 4). These foregoing facts specify that such interactions are very important in **I**–**III**, where they contribute significantly to molecular self-assembly processes.

The fluorescence properties of the Tibz ligand and complexes **I**–**III** have been studied in solid state at room temperature and the results were shown in Fig. 5. Under the 277 nm excitation, the strongest emission peak is observed at 344 nm for the Tibz ligand which may be attributed to ligand-centered

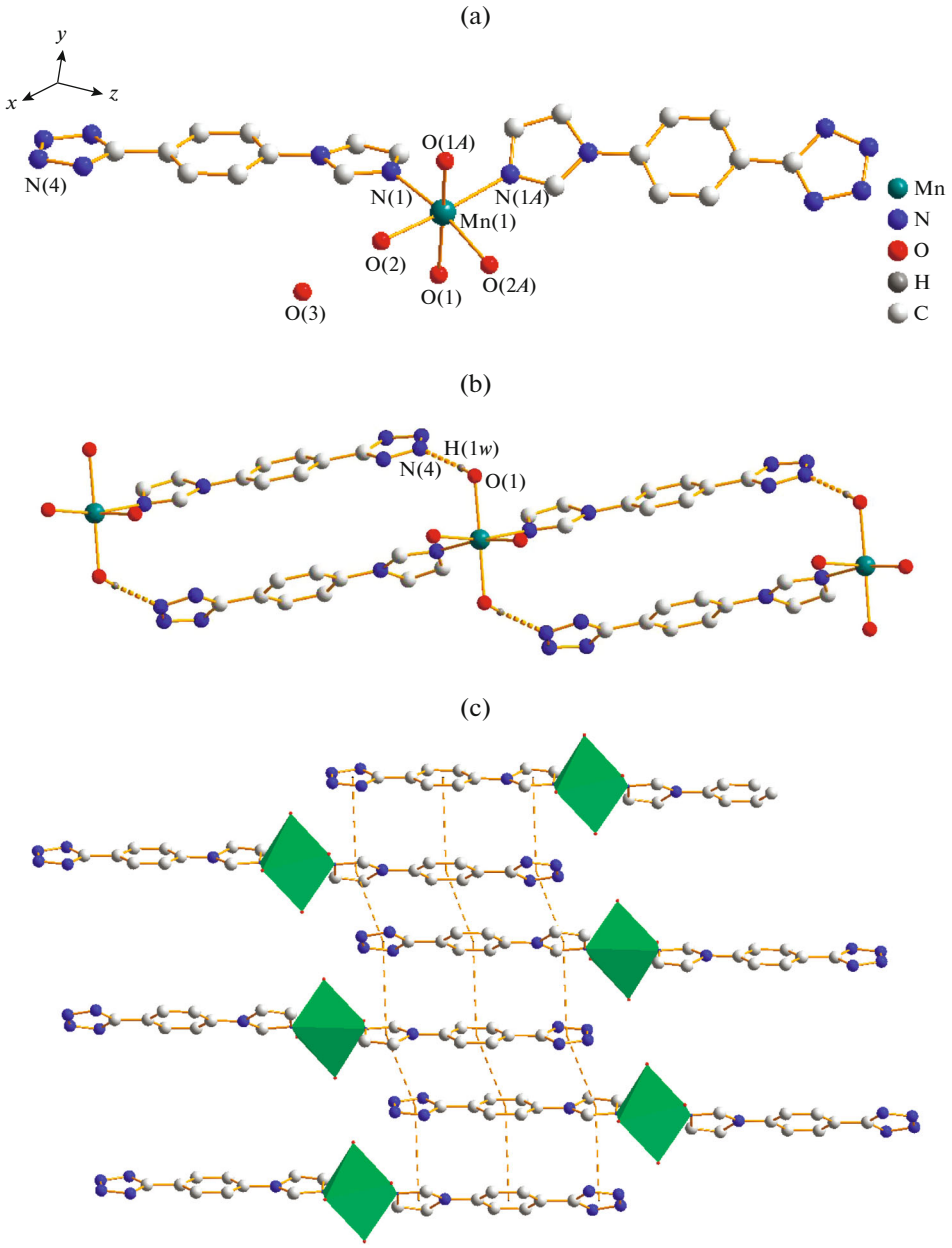

Fig. 2. The structure unit (a); the hydrogen-bonding interactions (b) and the π···π stacking interactions (c) of **II**.

electronic transitions. Compared to the ligand, polymer **I** shows a little blue shift of 14 nm and it gives relatively intense fluorescence at 330 nm under the same condition. Since the Cd^{2+} ions with d^{10} configuration are difficult to oxidize or to reduce, the emission bands of polymers of **I** is neither metal-to-ligand charge transfer (MLCT) nor ligand-tometal charge transfer (LMCT) in nature [17]. The intense fluorescence may be attributed to ligand-centered electronic transitions, which effectively strengthen the rigidity of the ligand and decreases the loss of energy by means of radiationless decay process of the intraligand emission excited state [18, 19]. The blue shift of emission bands for **I** may be due to the coordination interactions between the metals and the ligands [20, 21]. Different from polymer **I**, complex **II** gives weak fluorescence, which is red shifted relative to the free ligand. There are two intense emission maxima at 384 and 477 nm for complex **II**. The peak at 384 nm would be distributed to the intraligand emission, while the peak at 477 nm would be assigned to the emission of LMCT [19]. Complex **III** exhibits no fluorescence properties

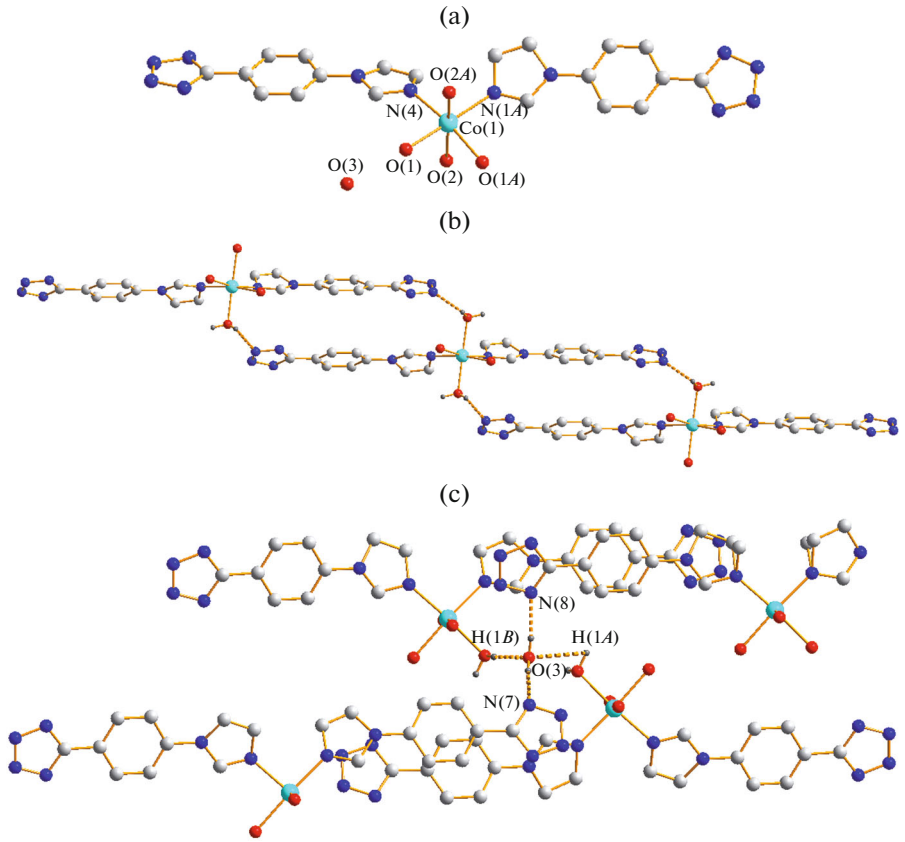

Fig. 3. The structure unit (a); the hydrogen-bonding interactions (b, c) of **III**. Hydrogen atoms are omitted for clarity.

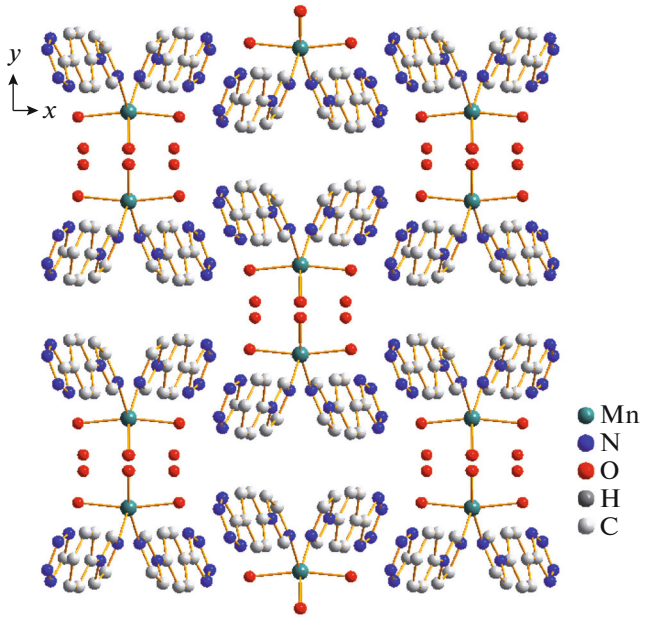

Fig. 4. The 3D packed structure of the complex **II** and **III**. Hydrogen atoms are omitted for clarity.

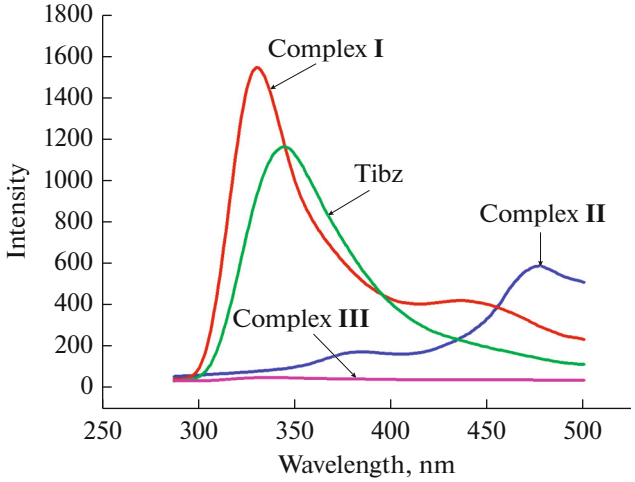

Fig. 5. Solid-state fluorescence spectra of free Tibz ligand and complexes **I**–**III** at room temperature.

comparing with the free ligand, it is visible that Co(II) shows fluorescence quenching for the Mbbz ligand. In conclusion, the polymer **I** may be excellent candidate for the exploration of fluorescent materials.

ACKNOWLEDGMENTS

This work was supported by the National Natural Science Foundation (nos. 21273205, J1210060, and 21543011) and Key scientific research projects of Henan Province (17A150020).

REFERENCES

1. Li, J.P., Li, X.F., Lu, H.J., et al., *Inorg. Chim. Acta*, 2012, vol. 384, p. 163.
2. Guo, Q.Q., Xu, C.Y., Zhao, B., et al., *Cryst. Growth Des.*, 2012, vol. 12, p. 5439.
3. Zhong, D.C., Lu, W.G., Jiang, L., et al., *Cryst. Growth Des.*, 2010, vol. 10, p. 739.
4. Li, Y., Xu, G., Zou, W.Q., et al., *Inorg. Chem.*, 2008, vol. 47, p. 7945.
5. Jin, S.W., Chen, W.Z., and Wang, D.Q., *J. Inorg. Organomet. Polym.*, 2007, vol. 17, p. 583.
6. Qiu, Y.C., Li, Y.H., Peng, G., et al., *Cryst. Growth Des.*, 2010, vol. 10, p. 1332.
7. Lama, P. and Bharadwaj, P.K., *Cryst. Growth Des.*, 2011, vol. 11, p. 5434.
8. Pachfule, P., Das, R., Poddar, P., and Banerjee, R., *Cryst. Growth Des.*, 2010, vol. 10, p. 2475.
9. Dincä, M., Yu, A.F., and Long, J.R., *J. Am. Chem. Soc.*, 2006, vol. 128, p. 8904.
10. Dong, P., Zhang, Q.K., Wang, F., et al., *Cryst. Growth Des.*, 2010, vol. 10, p. 3218.
11. Li, Z.X., Hu, T.L., Ma, H., et al., *Cryst. Growth Des.*, 2010, vol. 10, p. 1138.
12. Sheldrick, G.M., *SHELX-97*, Göttingen (Germany): Univ. of Göttingen, 1997.
13. Blake, A.J., Baum, G., Champness, N.R., et al., *J. Chem. Soc., Dalton Trans.*, 1996, p. 4379.
14. Li, J.P., Li, L.K., Hou, H.W., and Fan, Y.T., *J. Organomet. Chem.*, 2009, vol. 637, p. 1359.
15. Li, H.H., Ma, Y.J., and Zhao, Y.Q., *Transition Met. Chem.*, 2015, vol. 40, p. 21.
16. Zhao, N., Deng, Y.E., Liu, P., et al., *Transition Met. Chem.*, 2015, vol. 40, p. 11.
17. Lü, H.J., Mu, Y.J., Li, J.P., et al., *Inorg. Chim. Acta*, 2012, vol. 387, p. 450.
18. Wang, X.L., Qin, C., Wang, E.B., et al., *J. Mol. Struct.*, 2006, vol. 796, p. 172.
19. Zhang, L.Y., Liu, G.F., Zheng, S.L., et al., *Eur. J. Inorg. Chem.*, 2003, vol. 16, p. 2965.
20. Liu, F.L., Zhang, L.L., Wang, R.M., et al., *CrystEngComm*, 2014, vol. 16, p. 2917.
21. Liu, C.S., Wang, J.J., Chang, Z., et al., *CrystEngComm*, 2010, vol. 12, p. 1833.